

# Calculation of Weibull Strength Parameters and Batdorf Flow-Density Constants for Volume- and Surface-Flaw-Induced Fracture in Ceramics

Shantaram S. Pai  
*W.L. Tanksley and Associates, Inc.*  
*Lewis Research Center*  
*Cleveland, Ohio*

and

John P. Gyekenyesi  
*National Aeronautics and Space Administration*  
*Lewis Research Center*  
*Cleveland, Ohio*

(NASA-TM-100890) CALCULATION OF WEIBULL  
STRENGTH PARAMETERS AND BATDORF FLOW-DENSITY  
CONSTANTS FOR VOLUME- AND  
SURFACE-FLAW-INDUCED FRACTURE IN CERAMICS  
(NASA) 32 p

N89-12930

Unclas  
0174562

CSCL 20K G3/39

October 1988

**NASA**



CALCULATION OF WEIBULL STRENGTH PARAMETERS AND BATDORF FLAW-DENSITY  
CONSTANTS FOR VOLUME- AND SURFACE-FLAW-INDUCED  
FRACTURE IN CERAMICS

Shantaram S. Pai  
W.L. Tanksley & Associates, Inc.  
NASA Lewis Research Center  
Cleveland, Ohio 44135

and

John P. Gyekenyesi  
National Aeronautics and Space Administration  
Lewis Research Center  
Cleveland, Ohio 44135

SUMMARY

This paper describes the calculation of shape and scale parameters of the two-parameter Weibull distribution using the least-squares analysis and maximum likelihood methods for volume- and surface-flaw-induced fracture in ceramics with complete and censored samples. Detailed procedures are given for evaluating 90-percent confidence intervals for maximum likelihood estimates of shape and scale parameters, the unbiased estimates of the shape parameters, and the Weibull mean values and corresponding standard deviations. Furthermore, this paper describes the necessary steps for detecting outliers and for calculating the Kolmogorov-Smirnov and the Anderson-Darling goodness-of-fit statistics and 90-percent confidence bands about the Weibull distribution. It also shows how to calculate the Batdorf flaw-density constants by using the Weibull distribution statistical parameters. The techniques described have been verified with several example problems from the open literature, and have been coded in the Structural Ceramics Analysis and Reliability Evaluation (SCARE) design program.

E-4128

INTRODUCTION

The fracture behavior of ceramics differs considerably from that of metals. This is due to several factors: Little or no plastic deformation exists at crack tips in ceramics. They also possess lower fracture toughness, and sub-critical cracks grow under static or dynamic stresses, even in ambient environments. Ceramics are also not generally homogeneous. They may exhibit one or more types of defects with different distribution of sizes. The observed variability in ceramic strength is due to the presence of microcracks, the large range of flaw sizes, and the residual stresses arising from anisotropic contraction upon cooling. The design of load-bearing components using structural ceramics requires a complete understanding of the statistical nature of fracture in brittle materials.

The reliability and consistency of design strength data for ceramics is relatively poor when compared to the design data for materials like metals and plastics. The reason for this is that ceramics contain a large number of microcracks with various sizes and orientations which, along with residual

stresses from processing, cause a wide scatter in strength measurements. The great variation in strength of nominally identical specimens necessitates testing large numbers of samples to fully describe the failure phenomena. However, this poses a dilemma since the costs associated with testing equipment, specimen preparation, and precautions to ensure against damage of specimens are high. Thus, it is desirable to test an optimum, but relatively small, number of samples and to develop analytical procedures that yield material parameters with a high degree of accuracy.

A number of commonly used uniaxially loaded test specimens can be used to measure ceramic fast-fracture strength over a wide range of temperatures. These material characterization tests are derived from observed failure modes. The Army Specification (ref. 1) describes a test method for determining the flexure strength, or modulus of rupture (MOR), of brittle beam test specimens at ambient temperatures. Because of the scatter in observed strength values, many samples (typically 30 or more MOR bars for a specified temperature) are required. Fractography is required after fracture to separate flaw populations and to identify failure modes. The major advantages of this testing method include simple fixtures, low cost, and the ability to cut small test specimens out of component bulk.

However, an inherent weakness of flexure testing is that it emphasizes surface flaws relative to volume flaws. It also needs a greater order of magnitude of volume and area scaling between the specimen and the entire component geometry. To alleviate these problems, considerable effort has been focused on developing and using tensile fast-fracture tests. One form of these tests, recently developed at Oak Ridge National Laboratory (ORNL), uses a hydraulic self-aligning grip system (ref. 2). With the tensile test specimen, the entire gage material volume (which is generally much larger than in the flexure specimen) is loaded to the same maximum stress, and many successful tests produced near zero bending during monotonic tensile and cyclic tension-tension loading. With the emerging importance of ceramic tensile testing, the need for a smaller number of specimens, more advanced statistics for data reduction, and more selective testing than with MOR bars is evident.

Two main classes of fracture theory have been previously discussed in the literature. The first is derived from Griffith's flaw theory (refs. 3 and 4) which assumes the presence of cracks of specified sizes, shapes, and arbitrary orientations. There is always one crack with the least favorable orientation that causes failure. The second class consists of the weakest link theory (WLT) such as that of Weibull (ref. 5). This theory is purely statistical in nature. Failure in ceramics is due to a single weakest flaw where the local stress reaches a critical value. The inability of current inspection procedures to fully characterize flaws and the observed size effect on strength makes it necessary to use statistics and reliability analysis to predict failure of brittle material components.

Weibull (ref. 6) used the WLT to develop a probabilistic approach to account for the scatter in the fracture strength and the size effect of brittle materials. He assumed a unique cumulative strength distribution for the uniaxial fracture data obtained from simple test specimens. Weibull also adopted uniaxial fracture test parameters for calculating the failure probability in multidimensional stress states. The concept focuses on calculating the risk of rupture by averaging the normal tensile stress at any point in principal stress space. This approach is plausible, but rather arbitrary, and requires numerical modeling. Consequently, other models were proposed, and the most widely used model assumes that the principal stresses act independently (PIA)

(ref. 7). However, the PIA hypothesis may lead to unsafe estimates of failure probability because it neglects the effects of the interaction of combined local principal stresses (ref. 8).

Ceramic strength is well represented by the Weibull distribution which is fully characterized by its statistical parameters. Batdorf and Crose (ref. 9) proposed a new physically based statistical theory, which describes the material strength by a flaw-density function. This strength parameter is usually expressed in terms of a power function with appropriate flaw-density constants. It is then a simple matter to derive relationships between the Weibull parameters and the Batdorf flaw-density constants, so that the same material strength distributions are consistently obtained from both. Ruffin et al. (ref. 10) further extended the Batdorf statistical theories to investigate effects of different flaw geometries and mixed-mode fracture criteria on overall material reliability. Gyekenyesi and Nemeth (refs. 11 and 12) developed a public domain computer program incorporating the preceding theories which could be coupled to a general purpose finite element code such as MSC/NASTRAN (ref. 13) to predict the fast-fracture failure probability of ceramic components due to the presence of volume- and surface-type flaws.

The primary objective of this paper is to describe the estimation of the Weibull strength parameters and the Batdorf flaw-density constants for volume- and surface-flaw-induced fracture in ceramics. An extensive literature survey of various statistical estimation techniques was conducted and discussions were held with numerous researchers in the field. The goal was to quantify the uncertainty by using analytical methods. Many modern Weibull parameter estimators (ref. 14) are efficient and provide confidence intervals. Mann et al. (ref. 15) discuss moment estimators, least-square estimators, best least invariant estimators, and maximum likelihood estimators (MLE's). The evaluation of shape and scale parameters of the two-parameter Weibull distribution is explained initially in this paper by using the least-squares analysis (ref. 16). This method obtains, analytically, a unique line of best fit to describe the scatter in ceramic strength.

The MLE's have the smallest mean-square error, and Bain and Antle (ref. 17) found them to be the most efficient of the available methods. However, MLE's are highly biased for small samples, and, consequently, the MLE of the shape parameter is often unbiased to eliminate the deviation between the sample and true population. Important design criteria should not be derived from small sample sizes because uncertainty is known to increase as the number of samples decreases. Menon (ref. 18) describes the derivation of the maximum likelihood equations based on the assumption that the location parameter (threshold stress) is known. This method was further extended by Cohen (ref. 19) for singly censored samples. For small to moderately large sample sizes, distribution percentiles of the MLE's and unbiasing factors for the shape parameters have been computed and tabulated by Thoman et al. (ref. 20) through the use of Monte Carlo simulation procedures. Jeryan (ref. 21) developed a FORTRAN computer program to calculate the MLE's and other related statistical parameters for uncensored statistics. This paper summarizes the equations and procedures that are necessary for evaluating the MLE's of the shape and scale parameters, the Weibull mean values, and the corresponding standard deviations (ref. 22) by using theories of concurrent flaw distributions (ref. 23). The Weibull log likelihood equations for censored statistics were developed by Nelson (ref. 24) and used to calculate the MLE's for the censored data using Newton-Raphson iterative techniques. Procedures to evaluate

90-percent confidence intervals for MLE's of the shape and scale parameters and the unbiased estimates of the shape parameters for uncensored statistics are explained. No rigorous studies are known to the authors that evaluate the confidence intervals for MLE's of shape and scale parameters and the unbiased estimate of shape parameter for censored statistics. However, a Monte Carlo simulation is developed and tested for censored statistics, and the results are included in this paper.

An outlier is a data value that is far from the rest of the sample. Therefore, techniques are needed that detect outliers to reveal faulty products as well as to improve poor test data. Stefansky (ref. 25) describes a procedure for calculating critical values of the maximum normed residuals while testing for outliers. This technique is based upon the normal distribution, and its application to Weibull data is of concern. However, it was used by Neal et al. (ref. 26) to calculate the critical values for different significance levels. Sample size-dependent polynomial approximating functions have been developed to compute the critical values at 1-, 5-, and 10-percent significance levels, and these functions are described in this paper.

Many goodness-of-fit tests based on empirical distribution functions (EDF) have been extensively discussed by D'Agostino and Stephens (ref. 27). The EDF statistics measure the discrepancy between the EDF and a given distribution function. Five of the leading EDF statistics, including the Kolmogorov-Smirnov, the Cramér-von Mises, the Kuiper, the Watson, and the Anderson-Darling have been examined by Stephens (ref. 28). The Kolmogorov-Smirnov (K-S) test for goodness-of-fit is the most widely used in comparing an empirical distribution function with the distribution function of the hypothesized distribution for any finite sample sizes (ref. 29). Critical values of the maximum absolute difference between sample and population cumulative distributions have been tabulated by Massey (ref. 30). Percentage points in Kolmogorov-Smirnov statistics for probabilities from 0.01 through 0.20 were tabulated by Miller (ref. 31) for different sample sizes. This work was further extended by Amstadter (ref. 32) in evaluating values for probabilities from 0.30 through 0.99. The Anderson-Darling (A-D) statistic  $A^2$  (ref. 33) has proven more sensitive to the discrepancies in the tail regions between the EDF and the cumulative distribution function. Lewis (ref. 34) discusses the Anderson-Darling statistic for a fully specified distribution. This paper summarizes the steps to calculate the Kolmogorov-Smirnov and the Anderson-Darling goodness-of-fit statistics by using polynomial approximating functions to represent available tabular values from the literature.

Confidence bands (ref. 35) on the Weibull line can be calculated and plotted (ref. 36) for different confidence levels by making use of the mean and the standard deviation of the sample. This paper also explains the calculation of 90-percent confidence bands about the Weibull distribution.

Also, several currently used theories that can be used for calculating the Batdorf flaw-density constants from the Weibull distribution statistical parameters are selectively included in this paper. The most widely used model among these theories assumes that the cracks are shear-insensitive. Different relationships are obtained, however, if shear-sensitivity of the flaws is included. Finally, all the statistical techniques summarized here were verified with several example problems from the open literature, including the problem of deep-groove ball bearings (ref. 37) and the recently obtained Elektroschmelzwerk

Kempton (ESK) hot isostatically pressed HIPped silicon carbide (ref. 38) strength data.

## PROGRAM CAPABILITY AND DESCRIPTION

Volume- and surface-flaw-based reliability analysis has been implemented in both the SCARE1 and SCARE2 versions of the postprocessor program (refs. 11 and 12). The SCARE1 version of the code uses only elemental centroidal principal stresses to calculate the reliability for both volume and surface elements. In SCARE2, all linear or quadratic QUAD8 shell elements are further discretized into nine subelements with interpolated centroidal principal stresses and subelement areas used to perform reliability analysis. A similar discretization of brick volume elements into 27 subelements is performed for volume-flaw-based reliability studies. Both versions of SCARE have broad capabilities: Temperature-dependent multiple-flaw populations, statistical material parameters, several crack configurations, and a number of well-known fracture criteria can be specified. The existing architecture and basic computational elements of the programs were described in previous publications (refs. 11 and 12). Figure 1 shows the flowchart for calculation of shape and scale parameters of the two-parameter Weibull distribution using the least-squares analysis and the maximum likelihood methods for volume- and surface-flaw-induced fracture in ceramics with complete and censored samples, and the calculation of many other related statistical quantities. For convenience, these latest additions to the SCARE program can also be used independently of the MSC/NASTRAN postprocessing or without performing a reliability analysis.

## INPUT INFORMATION

SCARE input requirements are grouped into three major categories: the Master Control Deck, the Specimen Deck, and the Structures Deck. The details of the deck functions are explained in reference 11. For the calculation of shape and scale parameters of the two-parameter Weibull distribution, the data, which includes the fracture origins of the specimen, is entered in the Specimen Deck. Initially, for the statistical analysis of both complete and censored samples, each specimen fracture mode is observed by fractography or other means and identified as failed either by volume-flaw- or surface-flaw-induced fracture, V and S, respectively. If there is any uncertainty regarding a failure mode, it is input as an unknown failure mode U. The user can select any of the following three options of calculations for complete samples: Volume flaw analysis only, surface flaw analysis only, or both in one execution. For the last selection, two separate extreme fiber fracture stress data sets (which may be completely identical) are required for the analysis. The same user options are available for censored samples. When the third choice is selected, volume-flaw analysis will be done by treating surface-flaw and unknown-flaw failure mode data as suspended items; surface-flaw analysis will be done by treating the volume-flaw and unknown-mode data as censored information.

## OUTPUT INFORMATION

The details of SCARE output for a complete MSC/NASTRAN finite element analysis are discussed in previous publications (refs. 11 and 12). The output pertaining to the calculation of the Weibull strength parameters identifies the

method of solution, the control index used for experimental data, the number of specimens in each batch, and the temperature of each test. In addition, the output echoes the input values of all extreme fiber fracture stresses with proper failure mode identification. Any data value that is far from the rest of the sample is detected as an outlier, and its corresponding significance level (1, 5, and 10 percent) is printed. Furthermore, the biased and the unbiased values of the shape parameter, the specimen characteristic strength, the upper and lower bound values at 90-percent confidence level for both the shape parameter and the specimen characteristic strength, the specimen Weibull mean value, and the corresponding standard deviation are printed for each specified temperature. For censored statistics, the above values are generated first for volume-flaw analysis and, subsequently, for the surface-flaw analysis.

The Kolmogorov-Smirnov goodness-of-fit test is done for each data point, and the corresponding K-S statistic factors  $D^+$  and  $D^-$  are listed. Similarly, the K-S statistic for the overall population is printed along with the percentage significance level. This overall statistic is the absolute maximum of individual data  $D^+$  and  $D^-$  factors. For the Anderson-Darling goodness-of-fit test, the A-D statistic  $A^2$  is determined for the overall population, and its associated significance level is printed.

The next table of the output contains fracture stress data, the corresponding Weibull probability of failure values, the 90-percent upper- and lower-confidence band values about the Weibull line, and the median rank value for each data point. These statistical quantities are calculated by using either tabular values or approximating polynomial functions which are now incorporated into the SCARE program. Finally, the material parameters used in component reliability calculations are listed as a function of temperature. These include the biased Weibull modulus, the Batdorf crack-density coefficient, and the material Weibull scale parameter or unit volume and area characteristic strength, whichever is appropriate.

## THEORY

The weakest link theory of material strength considers not only the size effect and loading system, but also the variation in fracture strength due to intrinsic defect distributions. Paluszny and Wu (ref. 39) discuss evidence of adequate correlation between the reliability predictions of complex structures based on simple test bars using the Weibull methods and the experimental results. It is possible to use the Weibull distribution to model a broad range of instantaneous failure rates and also to represent several component failure mechanisms. It has been shown that experimental fracture strength data obtained from uniaxially loaded specimens is best approximated by the three-parameter Weibull distribution, defined by

$$P_f = 1 - \exp \left[ - \int_V \left( \frac{\sigma - \sigma_u}{\sigma_o} \right)^m dV \right] \quad (1)$$

where  $P_f$  is the probability of failure,  $\sigma$  is the applied tensile stress,  $\sigma_u$  is the threshold stress (location parameter usually taken as zero for ceramics),  $\sigma_o$  is the scale parameter with dimensions of stress  $\times$  (volume)<sup>1/m</sup>,  $m$  is the shape parameter (or the Weibull modulus) which measures the degree of strength variability, and  $V$  is the stressed volume. A similar equation can be written



for area-flaw-induced failure with area parameters replacing corresponding volume variables.

The location parameter is the value of  $\sigma$  below which the failure probability is zero. Similarly, the scale parameter corresponds to a stress level where 63.2 percent of specimens with unit volumes would fracture. The Weibull modulus is a measure of the strength dispersion, and as  $m$  increases, the strength becomes increasingly deterministic. Values of  $m = 3.44$  and  $m = 1$  give, respectively, the normal (approximate) and true exponential distribution curves as shown in figure 2. For large values of  $m$  ( $m \geq 40$ ), such as those obtained for ductile metals, the scale parameter corresponds to the material ultimate strength. Typically, for brittle materials, the Weibull parameters are determined from simple geometry and loading conditions, such as beams under flexure or cylindrical or flat specimens under uniform uniaxial tension.

### The Outliers

Before computing the estimates of the Weibull parameters, the available specimen fracture stress data must be carefully examined for outliers. Very often a data set may contain one or more values at the extremes which may not belong to the main trend of the overall population. Such data points or values are labeled as outliers. It is not always possible to notice these outliers without having a complete and thorough knowledge of the manner in which the data is obtained. However, from statistical computations, the outliers can be detected at different significance levels.

At the start of the outlier calculations, the sample mean  $\bar{\sigma}_f$  and the sample standard deviation  $s$  are calculated. From these values, the normed residuals  $\bar{r}_i$  for each sample are obtained as follows:

$$\bar{r}_i = \frac{\sigma_{fi} - \bar{\sigma}_f}{s}, \quad i = 1, 2, \dots, N \quad (2)$$

where  $N$  is the sample size. The normed residuals are normalized deviations of the data from the "center" of the data. The absolute maximum of the normed residual (MNR statistic) is compared to the critical value (CV), associated with the sample size. Critical values are calculated from the following equation:

$$CV = \frac{N - 1}{\sqrt{N}} \sqrt{\frac{t^2}{N - 2 + t^2}} \quad (3)$$

where  $t$  is the  $(1 - \alpha/2N)$  quantile of the  $t$ -distribution with  $N - 2$  degrees of freedom, and  $\alpha$  is the significance level. Separate polynomial approximating functions for sample sizes to 30 and above 30 have been developed for calculating CV at the appropriate significance level and are included in the SCARE program. These functions evaluate the critical values at 1-, 5-, and 10-percent significance levels. If the MNR statistic is smaller than the three critical values, then no outliers are detected. However, if the MNR is larger than at least one of the three critical values, the corresponding data value with the MNR statistic is detected as an outlier with the appropriate significance level. Once all the deviant points are detected, each potential outlier is retested against the remaining "good" data, and the results of this test are printed in the program output.

It is sometimes appropriate to omit the outliers and continue with the remaining analysis treating the reduced sample as a new sample or as a censored sample. But the rejection of outliers, strictly based on statistical analysis, can be misleading. Therefore, this technique of detecting the outliers should be used as a means of ascertaining the relative validity of the available data. Figure 3 shows the existence of a potential outlier in a data set for sintered  $\text{Si}_3\text{N}_4$  generated at NASA Lewis Research Center in cooperation with Oak Ridge National Laboratory. It appears that competing failure modes exist, and an outlier point is seen at the high-strength range of the data. Since fractography was not performed, the two Weibull distributions shown are assumed. Weibull parameters were only calculated for the combined distribution, which was treated as a complete sample, and its plot is also shown.

### Estimation of Statistical Material Parameters

The flexural test failure probability can be expressed in terms of the extreme fiber fracture stress  $\sigma_f$ , or MOR, using the Weibull form as

$$P_f = 1 - \exp[-C\sigma_f^m] = 1 - \exp[-C(\text{MOR})^m] \quad (4)$$

where  $C = (1/\sigma_0)^m$  and  $\sigma_0$  is the volume/area specimen characteristic strength, or characteristic modulus of rupture  $\text{MOR}_0$ . In equation (1),  $\sigma_0$  is based on unit volume; whereas in equation (4),  $\sigma_0$  includes effects of the specimen volume. A sample may only contain data from specimens that failed either from a surface flaw or from a volume flaw. Such a sample is usually called a complete sample. In some cases, specimens in a sample may not fail by one failure mode only, but by several competing failure modes. Such a situation exists in the case of concurrent flaw populations. Each specimen fracture origin is identified by fractography and then labelled as failed either due to a volume flaw or a surface flaw. For the computer input, these failure modes are denoted as V and S, respectively. Occasionally, some specimen fractures may not be identified directly due to uncertainty in the dominance of failure modes. Such data are grouped into an uncertain category and are denoted by U. Thus, the sample containing data from the mixture of failure modes, and sometimes inclusive of unknown failure modes, is referred to as a censored sample.

Many methods are available to estimate the statistical material parameters from experimental data. The success of the statistical approach depends on how well the probability function fits the actual material measurements, especially how accurate the value of  $m$  is. The two most popular models used to evaluate  $C$  and  $m$  are the least-squares analysis and the maximum likelihood methods. These statistical techniques are described in detail in the succeeding sections.

### The Least-Squares Analysis

The survival probability of a ceramic specimen in flexure strength testing is defined as

$$P_s = \exp[-C\sigma_f^m] \quad (5)$$

This equation can be linearized by taking the natural logarithm twice to obtain

$$\ln \left[ \ln \left( \frac{1}{P_s} \right) \right] = \ln \left[ \ln \left( \frac{1}{1 - P_f} \right) \right] = \ln C + m \ln \sigma_f \quad (6)$$

If the failure probability  $P_f$  is determined from conducting  $N$  tests and numbering the observed fracture stresses as  $\sigma_1, \sigma_2, \dots, \sigma_i, \dots, \sigma_N$  in an ascending order, then

$$P_f(\sigma_i) = \frac{i}{N + 1} \quad (7)$$

where  $i$  is the median rank. A more sophisticated treatment using median rank regression analysis gives the following result (ref. 36):

$$P_f(\sigma_i) = \frac{i - 0.3}{N + 0.4} \quad (8)$$

The difference between equations (7) and (8) becomes insignificant for large values of  $N$ . However, equation (8) is used in the remaining analysis as well as in the code. For the least-squares analysis, it is necessary to obtain the line of best fit with slope  $m$  and an intercept  $b$  which, as can be noted from equation (6), is equal to the natural log of  $C$ . By differentiating the sum of the squared residuals with respect to  $m$  and  $b$  separately, setting the results equal to zero, and then simultaneously solving for  $m$  and  $b$ , we obtain

$$b = \frac{\sum y_i \sum x_i^2 - \sum x_i y_i \sum x_i}{N \sum x_i^2 - \sum x_i \sum x_i} \quad (9)$$

$$m = \frac{N \sum x_i y_i - \sum x_i \sum y_i}{N \sum x_i^2 - \sum x_i \sum x_i} \quad (10)$$

where  $y_i$  and  $x_i$  are also obtained from equation (6). Thus, the material constants are calculated from known fracture stress data  $\sigma_{fi}$  at a specified temperature. With censored data, one cannot directly use the median rank regression analysis as given in equation (8) because of the presence of competing failure modes. To take into account the potential influence of the suspended items, Johnson (ref. 40) developed the rank increment technique, which is calculated from the following equation taken from reference 36:

$$\text{Rank increment} = \frac{(N + 1) - (\text{previous adjusted rank})}{1 + (\text{number of items beyond present suspended item})} \quad (11)$$

As mentioned earlier, all observed fracture stresses are arranged in ascending order, and rank increment values are calculated for each failure data by using equation (11). For volume-flaw analysis, all MOR's designated as  $V$ 's are considered as failure data; for surface-flaw analysis, the  $S$ 's are considered as failure data. According to the procedure discussed in reference 36, the new adjusted rank values are obtained by adding the rank increment value to the previously adjusted rank. These adjusted rank values are then

used to calculate the failure probability  $P_f$  by using median rank regression analysis (i.e., eq. (8)). Finally, the Weibull parameters  $m$  and  $C$  are obtained by solving equations (9) and (10), except that  $N$  now only includes the number of failed samples and not the total samples as in the case of complete (uncensored) data.

The least-squares analysis is a particular case of the maximum likelihood method, if we assume that the error is normally distributed with zero mean and constant variance. Somerville and Bean (ref. 41) compared the least-squares analysis and the maximum likelihood methods for different sets of conditions. The study concluded that when the data fits the Weibull distribution, both techniques produce substantially the same results. The least-squares analysis is most useful in situations where the underlying probability distribution is not clearly established, and it is more robust for minor departures from the Weibull distribution. In addition, the least-squares analysis may give better results for censored samples. While discussing the statistical approach to engineering design in ceramics, Davies (ref. 42) noted that the least-squares analysis gives better estimates of the parameter if a single anomalous high-strength value is present in the sample. King (ref. 43) determined the accuracy of the estimates of the Weibull parameters by using the prediction interval method, and he showed that the sampling distribution of the regression coefficients follows a  $t$ -distribution. This is true only if the error is normally distributed with zero mean and constant variance. Therefore, the least-squares analysis method is usually not suited to calculate confidence intervals and unbiasing factors and to take into account any uncertainty in the available data. For that reason, the maximum likelihood method has been extensively used in Weibull analysis and is discussed in detail here.

### The Maximum Likelihood Method

The maximum likelihood method is often used because of certain inherent properties. The likelihood equation from which the MLE's are obtained has a unique solution. In addition, as the sample size increases, the solution converges to the true values of the parameters, and, therefore, the solution is an asymptotically normal and asymptotically efficient estimate of the parameters. Jeryan (ref. 21) compared the maximum likelihood method to the method of moments and the pseudo-least-squares analysis for random sample sizes with assigned values for the Weibull parameters. It was concluded that the MLE of the Weibull slope showed the least bias and variance. According to Sonderman et al. (ref. 44), the maximum likelihood method is a wholly parametric technique, dependent on the form of the Weibull distribution to obtain its estimates. A comparative study (ref. 44) between the mean order, the hazard plotting, and the maximum likelihood estimates indicated that the MLE of the shape parameter was reasonably accurate for small samples. For complete as well as censored samples, no ranking functions or linear regression analysis are used while using the maximum likelihood method.

The likelihood equation is written by expressing the probability of obtaining the observed data. For the complete sample, the likelihood function is defined by

$$L = \prod_{i=1}^N f(\sigma_{fi}) = f(\sigma_{f1})f(\sigma_{f2}) \dots f(\sigma_{fN}) \quad (12)$$

In the analysis of failure of brittle materials subjected to uniaxial stress states, the Weibull probability density function is

$$f(\sigma_f) = \left(\frac{m}{\sigma_\theta}\right) \left(\frac{\sigma_f}{\sigma_\theta}\right)^{m-1} \exp\left[-\left(\frac{\sigma_f}{\sigma_\theta}\right)^m\right] \quad (13)$$

and the corresponding likelihood function is

$$L = \prod_{i=1}^N \left(\frac{m}{\sigma_\theta}\right) \left(\frac{\sigma_{fi}}{\sigma_\theta}\right)^{m-1} \exp\left[-\left(\frac{\sigma_{fi}}{\sigma_\theta}\right)^m\right] \quad (14)$$

In equation (14), the "likelihood" of the sample failure data  $\sigma_{f1}, \sigma_{f2}, \dots, \sigma_{fi}, \dots, \sigma_{fN}$  is a function of the Weibull parameters  $m$  and  $\sigma_\theta$ . The values of  $m$  and  $\sigma_\theta$  which maximize the likelihood function are determined by the maximum likelihood method. By differentiating the logarithm of the likelihood function with respect to  $m$  and  $\sigma_\theta$ , and then equating the resulting expressions to zero, we obtain the MLE's of  $m$  and  $\sigma_\theta$  by solving the resulting simultaneous equations.

In the complete sample case, the MLE of the shape parameter  $m$ , denoted by  $\hat{m}$ , should satisfy the following equation (ref. 36):

$$\frac{\sum_{i=1}^N (\sigma_{fi})^{\hat{m}} \ln(\sigma_{fi})}{\sum_{i=1}^N (\sigma_{fi})^{\hat{m}}} - \frac{1}{\hat{m}} \sum_{i=1}^N \ln(\sigma_{fi}) - \frac{1}{\hat{m}} = 0 \quad (15)$$

The Newton-Raphson iterative technique is used to solve equation (15) and to calculate  $\hat{m}$ . Furthermore, the MLE of the Weibull parameter  $\sigma_\theta$ , denoted by  $\hat{\sigma}_\theta$ , is evaluated by solving the following equation:

$$\hat{\sigma}_\theta = \left(\frac{\sum_{i=1}^N \sigma_{fi}^{\hat{m}}}{N}\right)^{1/\hat{m}} \quad (16)$$

However, if the sample is censored and the effect of a competing failure mode is taken into account, the following equation is solved by iterative techniques to obtain the value of  $\hat{m}$  (ref. 36):

$$\frac{\sum_{i=1}^N (\sigma_{fi})^{\hat{m}} \ln(\sigma_{fi})}{\sum_{i=1}^N (\sigma_{fi})^{\hat{m}}} - \frac{1}{\hat{m}} \sum_{i=1}^r \ln(\sigma_{fi}) - \frac{1}{\hat{m}} = 0 \quad (17)$$

In the preceding equation,  $r$  is the remaining number of specimens failed either by volume flaw or by surface flaw only. Finally,  $\hat{\sigma}_{\theta}$  is obtained from

$$\hat{\sigma}_{\theta} = \left( \frac{\sum_{i=1}^N \hat{\sigma}_{fi}^m}{r} \right)^{1/m} \quad (18)$$

In the previous cases, the MLE of the Weibull parameter  $C$ , as used in equation (4), is calculated by using the previously explained conversion technique. Incidentally, the MLE's of  $m$  and  $\sigma_{\theta}$  for the volume-flaw analysis are denoted by  $\hat{m}_V$  and  $\hat{\sigma}_{\theta V}$ ; for the surface-flaw analysis by  $\hat{m}_S$  and  $\hat{\sigma}_{\theta S}$ , respectively. Similarly, the parameter  $C$  is denoted as  $\hat{C}_V$  and  $\hat{C}_S$ .

As shown in figure 1, the least-squares analysis is always done first, irrespective of the method of analysis chosen. However, if the maximum likelihood method is selected, the initial estimate of the shape parameter for the iterative technique is set equal to the value of the parameter that is obtained from the least-squares analysis. This is convenient for computation, and the number of iterations in the Newton-Raphson technique is arbitrarily limited to 50. If no solution is found after 50 iterations, the maximum likelihood method is terminated, and the results from the least-squares analysis are used for further calculations in the program for both complete and censored samples.

#### Unbiasing Factors and Confidence Intervals

In the previously described maximum likelihood method, the MLE of the shape parameter is a biased estimate that depends on the number of specimens in the sample. Consequently, this parameter may not represent the true population. To minimize the deviation between the sample and the total population, the shape parameter estimate should be unbiased. Statistically, an estimator of any parameter is called an unbiased estimator if the mean of the estimators of its sampling distribution equals the value of the parameter itself. The non-zero difference between the estimator of the parameter and the parameter itself is called the bias of the estimator. Estimates are random variables, and a thorough understanding of the accuracy of the parameters estimation is needed. This is usually achieved by obtaining the confidence intervals of the distribution parameters. If the variable  $\theta$  and a quantity  $\theta^*$ , respectively, define the estimated and the true value of the parameter, then according to Siddall (ref. 45), the confidence interval is defined as an interval in  $\theta$  that will include the unknown value  $\theta^*$  with a probability  $\beta$ , where  $\beta$  is called the confidence level or confidence coefficient. The related uncertainty with the parameter estimate is based on a sample of data, and a different data set of the same size will yield different results. In general, the confidence intervals depend upon the sample data and not upon the parameters themselves. Consequently, the unbiasing factors, as well as the confidence intervals, play a major role in the analysis.

Thoman et al. (ref. 20) obtained the unbiasing factors for the MLE of  $m$  for complete samples by initially obtaining the MLE of  $m$  for a standard exponential density function, which is a two-parameter Weibull density function as

given in equation (13) with unit values of  $m$  and  $\sigma_0$ . The unbiasing factors for the MLE of  $m$  in reference 20 depend on sample size. The unbiased estimate of  $m$  is obtained by multiplying the biased estimate of  $m$  with the unbiasing factors. The percentage points of the distributions of MLE's were evaluated and then used to calculate the confidence intervals for MLE's at several confidence levels for complete samples (ref. 20). McLean and Fisher (ref. 46) discuss the uncertain nature of Weibull parameters estimations. Figures 4 and 5, taken from reference 1, show 90-percent confidence bounds for the Weibull modulus and the characteristic strength. As can be seen from the graphs, the error or the uncertainty in estimates from a small sample size is very large. The curves in figures 4 and 5 are obtained from tables 1 and 4 of reference 20.

A method of obtaining definite confidence intervals for censored samples has not yet been developed because of the additional complexity of competing failure modes. However, the effects of competing failure modes were examined through a Monte Carlo simulation on a limited trial basis by the authors. The investigation was performed by assigning two specified Weibull distributions as the parent populations, running a Monte Carlo simulation to mimic the competing failure modes, and recovering the MLE's for those trials, where a predetermined number of failures from a given mode occurred. It is estimated that 10 000 trials provide reasonable accuracy when calculating the 90-percent confidence limits of the parameters. Wetherhold (ref. 47) discusses in detail the statistical reasoning for the proper selection of the number of trials in the Monte Carlo simulation. With this method, the effect of sample size, including a given percentage of failure modes from the trial runs, indicated that the percentage points of the distribution asymptotically approached the complete sample case and depended on the number of failures for each failure mode.

It is clear from the preceding discussion that a knowledge of the upper and lower bound values of the MLE's of both parameters at any confidence level is necessary. This enables the user to estimate the uncertainty in the parameters as a function of the number of specimens. It is general practice to obtain these bounds at 90-percent confidence level, and, therefore, 5 and 95 percentage points of distribution of the MLE's of the parameters have been incorporated into the SCARE program, with data taken from reference 20. Furthermore, this also assures that if different data sets are used in the maximum likelihood method, then 90 percent of the time, the MLE's of the parameters will lie between the upper and lower bound values. The following equations describe the manner in which the different limit values are calculated at 90-percent confidence level.

$$\hat{m}_{UPP} = \frac{\hat{m}_{BIAS}}{\hat{m}_{5\%}} \quad (19)$$

$$\hat{m}_{LOW} = \frac{\hat{m}_{BIAS}}{\hat{m}_{95\%}} \quad (20)$$

$$\hat{\sigma}_{\theta \text{UPP}} = \frac{\hat{\sigma}_{\theta}}{\exp \left[ - \frac{\hat{\sigma}_{\theta 5\%}}{\hat{m}_{\text{BIAS}}} \right]} \quad (21)$$

$$\hat{\sigma}_{\theta \text{LOW}} = \frac{\hat{\sigma}_{\theta}}{\exp \left[ \frac{\hat{\sigma}_{\theta 95\%}}{\hat{m}_{\text{BIAS}}} \right]} \quad (22)$$

where a minus sign has been used in equation (21) to account for the data format. To calculate the upper and lower bound values, 5 and 95 percentage points of the distributions of the MLE's are used, respectively. All these values depend on the biased value of the MLE of the shape parameter, denoted by  $\hat{m}_{\text{BIAS}}$ . Jeryan (ref. 21) used the unbiased value of the shape parameter MLE to calculate the upper and lower bounds, while Thoman et al. (ref. 20) used the biased value as done here. Different approximating equations for these bounds can be found in reference 36 for complete samples.

#### The Weibull Mean and the Standard Deviation

After evaluating the MLE's of the Weibull parameters, the Weibull mean  $\mu$  and the standard deviation  $s$  can be obtained by using the following two equations (ref. 22):

$$\mu = \left( \hat{\sigma}_{\theta} \right) \Gamma \left( 1 + \frac{1}{\hat{m}_{\text{BIAS}}} \right) \quad (23)$$

$$s = \left\{ \left( \hat{\sigma}_{\theta} \right)^2 \left[ \Gamma \left( 1 + \frac{2}{\hat{m}_{\text{BIAS}}} \right) - \Gamma \left( 1 + \frac{1}{\hat{m}_{\text{BIAS}}} \right) \right] \right\}^{1/2} \quad (24)$$

where  $\Gamma$  denotes the gamma function. These equations are valid for both area- and volume-based flaw strength. Equations (23) and (24) indicate that as  $m$  increases, the mean of the distribution approaches the specimen characteristic strength, and the standard deviation approaches zero. We can also note that the specimen characteristic strength  $\sigma_{\theta}$  is related to the material scale parameter  $\sigma_0$  through the specimen effective volume/area relationship of  $\sigma_{0V} = \sigma_{\theta} V_e^{1/m_V}$  or  $\sigma_{0S} = \sigma_{\theta} S A_e^{1/m_S}$ .

#### Goodness-of-Fit Tests

Graphical techniques can often be used to determine whether or not a set of observations belongs to a population distribution. A discussion of these



methods for the Weibull and the lognormal distributions is given in reference 15. Subjective judgment is needed to test the goodness-of-fit of the data to the assumed distribution. In many instances, it is difficult to decide if the hypothesized distribution is valid. Therefore, classical statistics tests are used in verifying the available data.

In general, a statistic is a numerical value determined from a sample by using statistical computations. The difference between an empirical distribution function (EDF) and a given distribution function is called an EDF statistic. There are two major classes of statistics, and they differ in the manner in which the functional (vertical) difference between the two distribution functions is calculated. The supremum class statistic calculates the largest and smallest vertical differences between the two distribution functions. On the other hand, the quadratic class statistic measures the discrepancy between the two distributions through squared differences and the use of an appropriate weighting function.

The Kolmogorov-Smirnov goodness-of-fit statistic belongs to the supremum class and is very effective for small samples. To begin the K-S test, the sample is arranged in ascending order, and the EDF,  $F_N(x)$ , is obtained by using the following expressions (ref. 27):

$$\left. \begin{aligned} F_N(x) &= 0, & x < X_{(1)} \\ F_N(x) &= \frac{i}{N}, & X_{(i)} \leq x < X_{(i+1)}, \quad i = 1, 2, \dots, N-1 \\ F_N(x) &= 1, & X_{(N)} \leq x \end{aligned} \right\} \quad (25)$$

where  $x_1, x_2, \dots, x_N$  are from the sample. Figure 6 shows the step function calculated from the data. It is obvious that as  $x$  increases, the step function  $F_N(x)$  steps up as an individual sample observation is reached. For any  $x$ ,  $F_N(x)$  denotes the proportion of observations less than or equal to  $x$ ;  $F(x)$ , defined as the distribution function, is the probability of an observation less than or equal to  $x$ . The main intent of the K-S test is to calculate the well-known EDF statistic  $D$ , which is the maximum absolute vertical difference between the hypothesized cumulative distribution function  $F(x)$  and the EDF function  $F_N(x)$ . As shown in figure 6, the statistic  $D$  is obtained by initially evaluating two other statistics  $D^+$  and  $D^-$ , the largest vertical differences when  $F_N(x)$  is greater than  $F(x)$  and the largest vertical differences when  $F_N(x)$  is smaller than  $F(x)$ , respectively. In the SCARE program, all three statistics are calculated by using the following expressions (ref. 28):

$$\left. \begin{aligned} D^+ &= \left| \frac{i}{N} - F(x)_i \right| \\ D^- &= \left| F(x)_i - \frac{i-1}{N} \right| \quad i = 1, 2, \dots, N \\ D &= \max(D^+ \text{ or } D^-) \end{aligned} \right\} \quad (26)$$

For ceramics design, the  $F(x)_i$ 's are equal to  $P_f$ 's and are calculated by using equation (4). These are also referred to as the predicted failure probability for each fracture stress level and are evaluated by using the

biased values of the MLE's of the Weibull parameters. In the censored samples, the presence of two concurrent flaw populations makes it essential to calculate the cumulative survival probability first. This is accomplished by using equation (5) separately for volume and surface flaws, and then by multiplying the survival probabilities of the two concurrent flaw populations. Finally, the resultant predicted failure probability at each stress level is calculated by using the entire sample.

It is customary to express the EDF statistic  $D$  with an associated significance level  $\alpha$ , which is the probability of obtaining a higher maximum absolute difference assuming that the data follows the theoretical distribution. This probability is a function of  $D$  and the sample size  $N$ . Miller (ref. 31) described a general formulation for evaluating  $\alpha$  as follows:

$$\alpha = \frac{2}{\exp \left[ 2D^2 \frac{N}{\left(1 - \frac{0.5}{N}\right)^2} \right]} \quad (27)$$

For sample sizes of 30 or less, the values of  $\alpha$  obtained by using equation (27) are equal to the values given in reference 32. However, for sample sizes greater than 30, a separate formulation is used based on the discussion by Brunk (ref. 48), and is given by

$$\alpha = 2 \sum_{j=1}^{\infty} (-1)^{j-1} \exp[-2j^2 D^2] \quad (28)$$

or

$$\alpha = 1 - \frac{\sqrt{2\pi}}{D} \sum_{j=1}^{\infty} \exp \left[ -(2j-1)^2 \frac{\pi^2}{8D^2} \right]$$

In the SCARE program, the EDF statistics  $D^+$  or  $D^-$  are calculated for every specimen fracture stress level. Then the EDF statistic  $D$  and the associated significance level are determined for the total sample size. A higher value of  $\alpha$  indicates that the data fits the proposed distribution to a greater extent.

The Anderson-Darling statistic  $A^2$  belongs to the quadratic class and is a powerful statistic for goodness-of-fit measure. This approach measures the discrepancy between the EDF and the hypothesized cumulative distribution function by using the Cramér-von Mises formulation (ref. 27):

$$Q = N \int_{-\infty}^{\infty} \{F_N(x) - F(x)\}^2 \psi(x) dF(x) \quad (29)$$

where  $\psi(x)$  is a suitable weighting function applied to the squared difference. Anderson and Darling (ref. 33) introduced the  $A^2$  statistic by defining  $\psi(x) = \{[F(x)\{1 - F(x)\}]^{-1}$  in equation (29). This statistic is more suitable for identifying the discrepancies in the tail regions of the distribution. The concept of the probability integral transformation (PIT) is discussed in detail in

reference 27. In this procedure, a new random variable  $Z$ , which is uniformly distributed between 0 and 1, is introduced so that  $Z = F(X)$ , when  $F(x)$  is the true distribution of  $X$ . The  $Z_i$ 's are then arranged in ascending order and used to calculate the statistic  $A^2$  which is given by (ref. 27):

$$A^2 = -N - \left(\frac{1}{N}\right) \sum_{i=1}^N (2i - 1) \left[ \ln\{Z_{(i)}\} + \ln\{1 - Z_{(N+1-i)}\} \right] \quad (30)$$

In this case,  $Z_i$ 's are the predicted failure probabilities obtained from equation (4). It can be shown that for  $N > 3$ , the distribution of  $A^2$  is sufficiently independent of the sample size.

Lewis (ref. 34) discussed the asymptotic distribution and gave the values for the  $A^2$  statistic and the corresponding significance levels. These values are summarized in reference 27. We have developed several approximating polynomial functions to interpolate these values. If the  $A^2$  statistic is too large, the data should be rejected because the EDF fits the proposed distribution poorly. Otherwise, the significance level for the sample is calculated by using the  $A^2$  statistic and the corresponding polynomial function. Once again, the higher the value of  $\alpha$ , the better the data fits the proposed distribution.

#### Confidence Bands on the Weibull Line

Kanofsky and Srinivasan (ref. 35) described a method for constructing a confidence band on a continuous distribution function which may have normal, exponential, and many other functional forms. They introduced and defined the random variable  $\bar{L}$ , (the statistic  $\bar{L}$ ) as

$$\bar{L} = \max_x \left| F(x; \mu_p, \xi_p) - F(x; \bar{x}, s) \right| \quad (31)$$

where  $\mu_p$ ,  $\xi_p$ ,  $\bar{x}$ , and  $s$  are, respectively, the population mean, the population standard deviation, the sample mean, and the sample standard deviation. The population parameters  $\mu_p$  and  $\xi_p$  are unknown values. The sample is drawn from a continuous population distribution. In equation (31), the statistic  $\bar{L}$  is the maximum absolute difference between the two cumulative distribution functions. The distribution of the statistic  $\bar{L}$  is obtained in two stages: (1) The closed-form expressions for  $\bar{L}$  are derived. These expressions are functions of  $\bar{x}$  and  $s$ ; and (2) these expressions derive the distribution of  $\bar{L}$  by using Monte Carlo simulation. The random variable  $\bar{L}$  is then used to construct different percentage confidence bands on  $F(x; \mu_p, \xi_p)$  centered around  $F(x; \bar{x}, s)$ . This is similar to the use of the K-S statistic  $D$  in constructing a confidence band on any continuous cumulative distribution function centered around the EDF.

Abernethy et al. (ref. 36) extended the procedure by modeling the sample and its parent population with the Weibull distribution. Equation (32), with tabular data of  $K(N)$  from reference 36, is used in calculating the 90-percent confidence bands about the Weibull distribution for complete samples only. Thus,

$$\text{Confidence bands} = [F(x) - K(N), F(x) + K(N)] \quad (32)$$

where  $F(x)$  is the failure probability obtained by substituting the MLE's of the Weibull parameters in equation (4). The Kanofsky functions, denoted by  $K(N)$ , depend on the sample size. We have developed two sample-size-dependent approximate polynomial functions to interpolate these values, and we have incorporated them into the SCARE program. The two terms in equation (32) give the lower and upper 90-percent confidence band values about the Weibull distribution, respectively. Figure 7 indicates that for HIPped SiC flexure bars, the fracture stresses lie between the confidence bands about the Weibull line. The value of the statistic  $\bar{L}$  is 0.0829. It is also clear that the stress data fits a single Weibull distribution quite well.

### Batdorf-Weibull Statistical Parameters for Reliability Analysis

After evaluating the parameters  $C$  and  $m$  (either by the least-squares analysis or by the maximum likelihood method) using data from four-point bend bars or pure tensile specimens and after assessing the intrinsic uncertainties, the parameters required in reliability calculations are determined. The Weibull modulus  $m$  is directly used by all statistical fracture models and, consequently, requires no additional calculations. However, for the Weibull model the scale parameter  $\sigma_0$  is needed, while for the Batdorf approach the flaw-density coefficient  $k_B$  must be calculated. Both of these material constants are functions of  $m$ ,  $C$ , and specimen geometry. Details of evaluating  $\sigma_0$  and  $k_B$  are summarized elsewhere (refs. 11 and 12), but the results are included here to show how the two sets of constants are related. For volume-flaw analysis, using quadrant ( $L_1 = 2L_2$ ), four-point MOR bar data with known geometry,  $\sigma_{0V}$  is calculated from

$$\sigma_{0V} = \left[ \left( \frac{wh}{2} \right) \frac{(L_1 + m_V L_2)}{C_V (m_V + 1)^2} \right]^{1/m_V} \quad (33)$$

For shear-insensitive fracture criterion,  $k_{BV}$  is obtained from

$$k_{BV} = (2m_V + 1) \left[ \frac{2C_V (m_V + 1)^2}{wh(L_1 + m_V L_2)} \right] \quad (34)$$

where  $w$  is the width of the rectangular beam,  $h$  is the height, and  $L_1$  and  $L_2$  are, respectively, the lengths between symmetrically placed outer loads and inner loads. By comparing equations (33) and (34), we concluded that when the normal stress failure criterion is used,  $k_{BV}$  and  $\sigma_{0V}$  are related by

$$k_{BV} = (2m_V + 1) \left( \frac{1}{\sigma_{0V}} \right)^{m_V} \quad (35)$$

However, for shear-sensitive fracture criteria when crack shape must also be specified, the format of equation (35) changes according to the criterion and the crack shape selected. In addition, if we note that  $C_V = V_e \sigma_0^{-m_V}$ , where  $V_e$  is the effective volume, equation (33) can be solved for  $V_e$  to obtain

$$V_e = \left(\frac{wh}{2}\right) \frac{(L_1 + m_V L_2)}{(m_V + 1)^2} = \frac{(m_V + 2)}{4(m_V + 1)^2} V \quad (36)$$

where  $V = whL_1$ , the total volume of the specimen. For uniaxial tensile loading, the effective volume is equal to the specimen gage volume  $V_g$ , which is at the same time the total specimen volume  $V$  of interest in that test.

In surface-flaw-based reliability analysis, the effective area  $A_e$  for a rectangular beam in four-point bending is (ref. 12)

$$A_e = \left\{ \left[ \frac{\left(\frac{L_2}{L_1}\right)^{m_S} + 1}{2(m_S + 1)^2} \left( \frac{m_S w}{w + h} + 1 \right) \right] \right\} 2L_1(w + h) \quad (37)$$

In terms of  $A_e$  and the extreme fiber fracture stress  $\sigma_f$ , we can rewrite equation (4) as

$$P_{fS} = 1 - \exp \left[ -A_e \left( \frac{\sigma_f}{\sigma_{oS}} \right)^{m_S} \right] \quad (38)$$

Comparing equations (4) and (38) gives

$$\sigma_{oS} = \left( \frac{A_e}{C_S} \right)^{1/m_S} \quad (39)$$

Finally, the Batdorf surface-crack density coefficient  $k_{BS}$  is calculated from (ref. 12)

$$k_{BS} = \frac{2^{3/2-m_S}}{A_e} C_S^{m_S} (m_S - 1) \int_{-1}^1 (1 + \eta)^{m_S-2} (1 - \eta)^{1/2} d\eta \quad (40)$$

where  $\eta = [(\sigma_f/\sigma_{Cr}) - 1]$ . Equation (40) can be integrated numerically by using Gaussian quadratures to evaluate  $k_{BS}$ . In pure tensile loading, the effective area in equations (39) and (40) is just equal to the specimen gage area  $A_g$ .

Recently, it has been noted that equation (40) can be evaluated in closed form to obtain

$$k_{BS} = \frac{m_S \sqrt{\pi} \Gamma(m_S)}{\Gamma(m_S + \frac{1}{2})} \left( \frac{1}{\sigma_{oS}} \right)^{m_S} \quad (41)$$

where  $\Gamma$  is the gamma function, and  $A_e$  and  $C_S$  were eliminated through the use of equation (39). The last term in equation (41) is often referred to as the uniaxial Weibull surface-crack coefficient, that is  $k_{WS} = \sigma_{oS}^{m_S}$ . To derive equations (40) and (41), we have assumed that the material is shear-insensitive. Under this condition, the Batdorf flaw-density constant  $k_{BS}$  is identical with the polyaxial Weibull coefficient  $k_{WPS}$  that can be obtained from using the Weibull normal-stress-averaging method. In the previous equations, the parameters  $m$  and  $C$  are the biased MLE's of the parameters themselves for both volume- and surface-flaw fracture characterization. In the SCARE computer program, equations (35) and (41) are used to calculate the material constants  $k_{BV}$  and  $k_{BS}$ , respectively, for the Batdorf shear-insensitive model.

However, if we select shear-sensitive fracture criteria to convert MOR bar or tensile fracture data into Batdorf-model crack-function coefficients, equations (35) and (41) will no longer apply. As an example, if we choose to model both volume and surface imperfections as Griffith cracks (usually conservative but not a good representation of flaws) and apply the total strain energy-release-rate criterion (self-similar crack extension) to predict impending fracture, the following equations are obtained:

$$k_{BV} = (m_V + 1) \left( \frac{1}{\sigma_{oV}} \right)^{m_V} \quad (42)$$

$$k_{BS} = \frac{m_S \sqrt{\pi} \Gamma\left(\frac{m_S}{2}\right)}{2 \Gamma\left(\frac{m_S + 1}{2}\right)} \left( \frac{1}{\sigma_{oS}} \right)^{m_S} \quad (43)$$

In deriving equations (42) and (43), collinear crack growth was assumed, and the results for typical values of  $m_V$  and  $m_S$  ( $m_V = m_S = 10.0$ ) give considerably smaller Batdorf flaw-density coefficients than those obtained from using the previous shear-insensitive theory. Consequently, failure probabilities for a given structure will decrease when equations (42) and (43) are used to characterize a material. Presently, a new effort is underway to derive closed-form solutions for the Batdorf coefficients by using out-of-plane crack extension criterion (ref. 49) with the penny-shaped crack (PSC) for volume flaws and the semicircular-edge crack for surface flaws. In the SCARE program, all these user options are included, and results are obtained through numerical procedures as in multidimensional stress states. It is important to note that using the Batdorf theory requires no new material test procedures and data. The knowledge of Weibull parameters  $m$  and  $\sigma_o$ , whether performing volume- or surface-flaw analysis, is adequate for all fast-fracture-failure calculations.

## DISCUSSION AND EXAMPLES

Several benchmark problems were analyzed from the open literature to calculate the material strength parameters. The MLE's of the Weibull parameters for the results of endurance tests of nearly 5 000 deep-groove ball bearings (ref. 37) were compared and are included in table I. The test results, in millions of revolutions, for 23 ball bearings were 17.88, 28.92, 33.00, 41.52,

42.12, 45.60, 48.48, 51.84, 51.96, 54.12, 55.56, 67.80, 68.64, 68.64, 68.88, 84.12, 93.12, 98.64, 105.12, 105.84, 127.92, 128.04, 173.40. Table I shows that the SCARE results are very close to that of Thoman et al. (ref. 20) and Lieblein and Zelen (ref. 37). For the preceding data set, the data value 173.40 is detected as an outlier at 1-percent significance level, the K-S statistic  $D$  is 0.1512 (fig. 6) at 66.7-percent probability level, and the A-D statistic  $A^2$  is 0.3288 at 91.5-percent probability level. This indicates that the data fits the hypothesized Weibull distribution quite well, especially since only 23 specimens are available in this sample.

The IEA Annex II agreement (ref. 38) focuses on cooperative research and development among several countries in the areas of structural ceramics. In November 1986, 400 HIPped SiC flexure bars from Germany were distributed by ORNL to the five U.S. participating laboratories, including NASA Lewis Research Center. The bars were fractured at these laboratories, and the fracture stress data sets were returned to ORNL as complete data without censoring for different failure modes. Details of the statistical analyses of these data sets are given in reference 38. The results of 80 SiC flexure bars tested at NASA Lewis were obtained, (table II) and analyzed by using our present enhancement to SCARE to calculate the MLE's of the Weibull parameters. According to the results in table III, the Weibull parameter values from SCARE match two other predictions very well and are in reasonable agreement with the other three predictions, despite the use of different test operators, test equipment, and software to reduce the data. The only difference between the SCARE and NASA Lewis data shown is the use of different software to calculate  $m$  and  $\sigma_0$ . ASEA Cerama HIPped Si<sub>3</sub>N<sub>4</sub> bars (ref. 38) from Sweden were also fractured at NASA Lewis, and, subsequently, the shape parameter value was independently obtained by using the least-squares analysis and the maximum likelihood methods. This data set has also been analyzed by using the SCARE estimators, and the comparison of results is shown in table IV. Finally, several proprietary Monte Carlo simulated distributions were analyzed, and the results were consistently in good agreement with those from other estimators.

## CONCLUSIONS

The general purpose, statistical, fast-fracture probability code SCARE has been enhanced to include the details of calculating the shape and scale parameters of the two-parameter Weibull distribution by using the least-squares analysis and the maximum likelihood methods for volume- and surface-flaw-induced fracture in ceramics. If any sample, complete or censored, fits the Weibull distribution, then these two methods are the most powerful and appropriate techniques for obtaining the Weibull parameter estimates. In addition, for complete samples only, the maximum likelihood method enables the user to evaluate 90-percent confidence intervals for the MLE's of the Weibull parameters and the unbiased estimates of the shape parameter. Therefore, further research is needed in developing confidence intervals and the unbiasing factors for censored samples. The current addition to SCARE describes how to detect outliers and how to calculate Kolmogorov-Smirnov and Anderson-Darling goodness-of-fit test statistics and the 90-percent confidence bands about the Weibull distribution.

The fracture data of a material, especially in the limited-strength range used in laboratory tests, may fit many distributions other than the Weibull distribution. However, prior experience with ceramics suggests that the Weibull distribution is the best distribution to fit the failure data. Fractography is essential for proper identification of flaw origins. Independent Weibull equations are used for volume- and surface-flaw-based reliability analyses. In addition, the Weibull parameters are used to calculate the Batdorf flaw-density constants for shear-insensitive cracks using closed-form solutions. These constants are calculated for both volume- and surface-flaw-based reliability analysis. For shear-sensitive cracks, however, numerical procedures are used in the SCARE code, just as in multidimensional stress states.



## REFERENCES

1. Baratta, F.I.; Matthews, W.T.; and Quinn, G.D.: Errors Associated with Flexure Testing of Brittle Materials. MTL-TR-87-35, U.S. Army Materials Technology Laboratory, Watertown, MA., July 1987.
2. Liu, K.C.; and Brinkman, C.R.: Tensile Cyclic Fatigue of Structural Ceramics. Proceedings of the 23rd Automotive Technology Development Contractors' Coordination Meeting, Society of Automotive Engineers, Warrendale, PA, 1986, pp. 279-284.
3. Griffith, A.A.: The Phenomena of Rupture and Flow in Solids. Philos. Trans. Roy. Soc. A, vol. 221, 1921, pp. 163-198.
4. Griffith, A.A.: The Theory of Rupture. Proceedings of the 1st International Congress for Applied Mechanics, C.B. Biezeno and J.M. Burgers, eds., Delft, 1924, pp. 55-63.
5. Weibull, W.: The Phenomenon of Rupture in Solids. Ingeniors Ventenskaps Akademien Handlingar, No. 153, 1939, pp. 5-55.
6. Weibull, W.: A Statistical Theory of the Strength of Materials. Ingeniors Ventenskaps Akademien Handlingar, No. 151, 1939, pp. 5-45.
7. Freudenthal, A.M.: Statistical Approach to Brittle Fracture. Fracture, An Advanced Treatise, Vol. 2: Mathematical Fundamentals, H. Liebowitz, ed., Academic Press, 1968, pp. 591-619.
8. Batdorf, S.B.: Some Approximate Treatments of Fracture Statistics for Polyaxial Tension. Int. J. Fract., vol. 13, no. 1, Feb. 1977, pp. 5-11.
9. Batdorf, S.B.; and Crose, J.G.: A Statistical Theory for the Fracture of Brittle Structures Subjected to Nonuniform Polyaxial Stresses. J. Appl. Mech., vol. 41, no. 2, June 1974, pp. 459-464.
10. Rufin, A.C.; Samos, D.R.; and Bollard, R.J.H.: Statistical Failure Prediction Models for Brittle Materials. AIAA J., vol. 22, no. 1, Jan. 1984, pp. 135-140.
11. Gyekenyesi, J.P.: SCARE: A Postprocessor Program to MSC/NASTRAN for the Reliability Analysis of Structural Ceramic Components. J. Eng. Gas Turbines Power, vol. 108, no. 3, July 1986, pp. 540-546.
12. Gyekenyesi, J.P.; and Nemeth, N.N.: Surface Flaw Reliability Analysis of Ceramic Components with the SCARE Finite Element Postprocessor Program. J. Eng. Gas Turbines Power, vol. 109, No. 3, July 1987, pp. 274-281.
13. Schaeffer, H.G.: MSC/NASTRAN Primer: Static and Normal Modes Analysis, Rev. Ed., Schaeffer Analysis Inc., Mount Vernon, NH, 1982.
14. Berger, R.W.; and Lawrence, K.: Estimating Weibull Parameters by Linear and Nonlinear Regression. Technometrics, vol. 16, no. 4, Nov. 1974, pp. 617-619.

15. Mann, N.R.; Schafer, R.E.; and Singpurwalla, N.D.: *Methods for Statistical Analysis of Reliability and Life Data*. John Wiley, New York, 1974.
16. Jayatilaka, A.S.: *Fracture of Engineering Brittle Materials*. Applied Science Publishers Ltd., London, 1979, pp. 195-208.
17. Bain, L.J.; and Antle, C.E.: Estimation of Parameters in the Weibull Distribution. *Technometrics*, vol. 9, no. 4, Nov. 1967, pp. 621-627.
18. Menon, M.V.: Estimation of the Shape and Scale Parameters of the Weibull Distribution. *Technometrics*, vol. 5, no. 2, May 1963, pp. 175-182.
19. Cohen, A.C.: Maximum Likelihood Estimation in the Weibull Distribution Based on Complete and on Censored Samples. *Technometrics*, vol. 7, no. 4, Nov. 1965, pp. 579-588.
20. Thoman, D.R.; Bain, L.J.; and Antle, C.E.: Inferences on the Parameters of the Weibull Distribution. *Technometrics*, vol. 11, no. 3, Aug. 1969, pp. 445-460.
21. Jeryan, R.A.: Use of Statistics in Ceramic Design and Evaluation, *Ceramics for High Performance Applications II*, J.J. Burke, E.N. Leno and R.N. Katz, eds., Brook Hill Publishing Company, Columbus, OH, 1978, pp. 35-51.
22. Kapur, K.C.; and Lamberson, L.R.: *Reliability in Engineering Design*. John Wiley, New York, 1977, pp. 291-295.
23. Johnson, C.A.: Fracture Statistics of Multiple Flaw Distributions. *Fracture Mechanics of Ceramics*, Vol. 5, R.C. Bradt, et al., eds., 1983, pp. 365-386.
24. Nelson, W.: *Applied Life Data Analysis*. Wiley, 1982, pp. 333-395.
25. Stefansky, W.: Rejecting Outliers in Factorial Designs. *Technometrics*, vol. 14, no. 2, May 1972, pp. 469-479.
26. Neal, D.; Vangel, M.; and Todt, F.: Statistical Analysis of Mechanical Properties. *Engineered Materials Handbook*, Vol. 1, Composites, ASM International, Metals Park, OH, 1987, pp. 302-307.
27. D'Agostino, R.B.; and Stephens, M.A.: *Goodness-of-Fit Techniques*. Marcel Dekker, 1986, pp. 97-193.
28. Stephens, M.A.: EDF Statistics for Goodness-of-Fit and Some Comparisons. *J. Am. Stat. Assoc.*, vol. 69, no. 347, Sept. 1974, pp. 730-737.
29. Birnbaum, Z.W.: Numerical Tabulation of the Distribution of Kolmogorov's Statistic for Finite Sample Size. *J. Am. Stat. Assoc.*, vol. 47, 1952, pp. 425-441.
30. Massey, F.J., Jr.: The Kolmogorov-Smirnov Test for Goodness-of-Fit. *J. Am. Stat. Assoc.*, vol. 46, 1951, pp. 68-77.
31. Miller, L.H.: Table of Percentage Points of Kolmogorov Statistics. *J. Am. Stat. Assoc.*, vol. 51, no. 273, 1956, pp. 111-121.

32. Amstadter, B.: Reliability Mathematics, Fundamentals, Practices, Procedures. McGraw-Hill, 1971, pp. 76-79.
33. Anderson, T.W.; and Darling, D.A.: A Test of Goodness-of-Fit. J. Am. Stat. Assoc., vol. 49, 1954, pp. 765-769.
34. Lewis, P.A.W.: Distribution of the Anderson-Darling Statistic. Ann. Math. Stat., vol. 32, 1961, pp. 1118-1124.
35. Kanofsky, P.; and Srinivasan, R.: An Approach to the Construction of Parametric Confidence Bands on Cumulative Distribution Functions. Biometrika, vol. 59, no. 3, 1972, pp. 623-631.
36. Abernethy, R.B., et al.: Weibull Analysis Handbook. PWA/GPD-FR-17579, Pratt and Whitney Aircraft, West Palm Beach, FL, Nov. 1983. (Avail. NTIS, AD-A143100.)
37. Lieblein, J.; and Zelen, M.: Statistical Investigation of the Fatigue Life of Deep-Groove Ball Bearings. J. Res. Nat. Bur. Stand., vol. 57, no. 5, Nov. 1956, pp. 273-316.
38. Tennery, V.J.: IEA Annex 11 Management, Subtask 4 Results. Ceramic Technology for Advanced Heat Engines Project, Semiannual Progress Report Oct. 1986-Mar. 1987, Martin Marietta Energy Systems Inc., Oak Ridge, TN.
39. Paluszny, A.; and Wu, W.: Probabilistic Aspects of Designing with Ceramics. J. Eng. Power, vol. 99, no. 4, Oct. 1977, pp. 617-630.
40. Johnson, L.G.: The Statistical Treatment of Fatigue Experiments. Elsevier Publishing Co., 1964, pp. 37-41.
41. Somerville, P.N.; and Bean, S.J.: A Comparison of Maximum Likelihood and Least Squares for the Estimation of a Cumulative Distribution. J. Stat. Comput. Simul., vol. 14, nos. 3-4, 1982, pp. 229-239.
42. Davies, D.G.S.: The Statistical Approach to Engineering Design in Ceramics. Proc. Br. Ceram. Soc., no. 22, 1973, pp. 429-452.
43. King, R.L.: The Determination of Design Allowable Properties for Advanced Composite Materials. GEC J. Research, vol. 5, no. 2, 1987, pp. 76-87.
44. Sonderman, D., et al.: Maximum Likelihood Estimation Techniques for Concurrent Flaw Subpopulations. J. Mater. Sci., vol. 20, no. 1, Jan. 1985, pp. 207-212.
45. Sidall, J.N.: Probabilistic Engineering Design. Marcel Dekker, 1983, pp. 509-514.
46. McLean, A.F.; and Fisher, E.A.: Brittle Materials Design, High Temperature Gas Turbine. AMMRC-CTR-77-20, Aug. 1977. (Avail. NTIS, AD-B023566.)
47. Wetherhold, R.C.: Statistics of Fracture of Composite Materials Under Multiaxial Loading. Doctoral Thesis, The University of Delaware, 1983.

48. Brunk, H.D.: An Introduction to Mathematical Statistics. Third Ed., Xerox College Publishing, Lexington, MA, 1975, pp. 445-447.
49. Shetty, D.K.: Mixed-Mode Fracture Criteria for Reliability Analysis and Design with Structural Ceramics. J. Eng. Gas Turbines Power, vol. 109, no. 3, July 1987, pp. 282-289.

TABLE I. - ENDURANCE TESTS OF DEEP-GROOVE  
BALL BEARINGS

[All estimates are biased estimates.]

Parameter estimates	Maximum likelihood estimates (MLE) of -	
	Weibull modulus, $m$	Characteristic strength, $\sigma_{\theta}$ , Revolution $\times 10^{-6}$
Lieblein and Zelen (ref. 37)	2.230	80.00
Thoman et al. (ref. 20)	2.102	81.99
SCARE (refs. 11 and 12)	2.103	81.88

TABLE II. - EXTREME FIBER FRACTURE STRESSES OF ELECKTROSCHMELZWERK KEMPTEN (ESK)  
HIPped SILICON CARBIDE (SiC) BARS

Flexure bar	Strength, MPa	Flexure bar	Strength, MPa	Flexure bar	Strength, MPa	Flexure bar	Strength, MPa
1	281.2	21	446.2	41	516.2	61	588.6
2	291.0	22	451.5	42	519.8	62	591.0
3	358.2	23	452.1	43	527.6	63	591.0
4	385.4	24	452.7	44	530.7	64	593.3
5	389.0	25	470.4	45	530.7	65	598.7
6	390.8	26	474.1	46	545.7	66	599.6
7	391.8	27	475.5	47	548.8	67	610.0
8	402.8	28	475.5	48	552.7	68	612.7
9	412.5	29	479.2	49	559.6	69	619.9
10	413.3	30	483.5	50	562.4	70	619.9
11	413.9	31	484.8	51	563.3	71	622.2
12	417.8	32	486.2	52	566.1	72	622.3
13	418.2	33	488.6	53	566.5	73	640.5
14	426.9	34	492.5	54	570.1	74	649.0
15	437.6	35	493.2	55	572.8	75	657.2
16	440.0	36	496.0	56	575.0	76	660.0
17	441.0	37	505.7	57	576.1	77	664.3
18	442.5	38	511.9	58	580.0	78	673.5
19	443.8	39	512.5	59	582.6	79	673.9
20	444.9	40	513.8	60	588.0	80	725.3

TABLE III. - WEIBULL PARAMETERS FOR FLEXURE  
STRENGTH DATA SET OF ESK HIPped  
SILICON CARBIDE BARS  
[All estimates are biased estimates.]

Fracture data set	Maximum likelihood estimates (MLE) of -	
	Weibull modulus, m	Characteristic strength, $\sigma_0$ , MPa
GTE Laboratories	7.16	541.17
Sohio	6.82	517.01
Allison	4.91	508.88
NASA Lewis	6.59	556.72
Garrett	6.60	554.01
SCARE	6.49	555.80

TABLE IV. - WEIBULL PARAMETERS FOR FLEXURE STRENGTH DATA SET OF ASEA CERAMA HIPped SILICON NITRIDE BARS  
[All estimates are biased estimates.]

Parameter estimate	Least squares analysis method		Maximum likelihood method	
	Estimate of Weibull modulus, $m$	Estimate of characteristic strength, $\sigma_{\theta}$ , MPa	MLE of Weibull modulus, $m$	MLE of characteristic strength, $\sigma_{\theta}$ , MPa
NASA Lewis SCARE	12.1 11.74	Not available 690.5	13.4 13.38	686.0 686.2

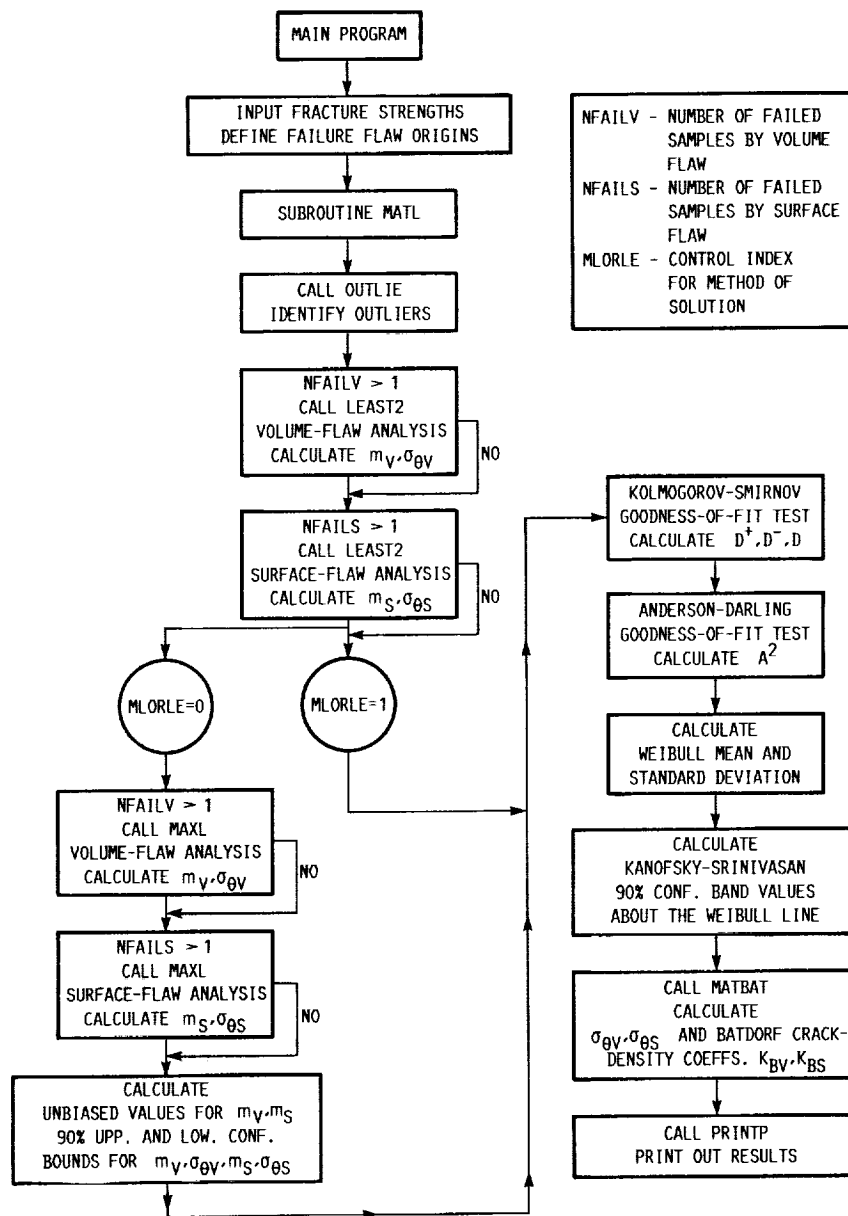


FIGURE 1. - FLOWCHART FOR MATERIAL STATISTICAL STRENGTH PARAMETERS CALCULATIONS.

ORIGINAL PAGE IS  
OF POOR QUALITY

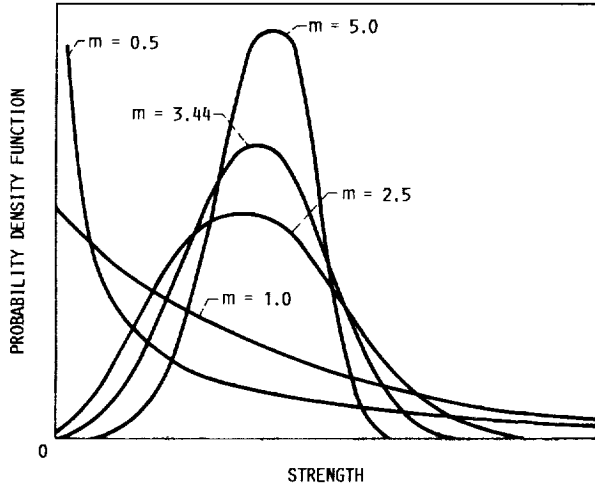


FIGURE 2. - PROBABILITY DENSITY FUNCTION-STRENGTH DIAGRAM FOR VARIOUS VALUES OF THE WEIBULL SHAPE PARAMETER.

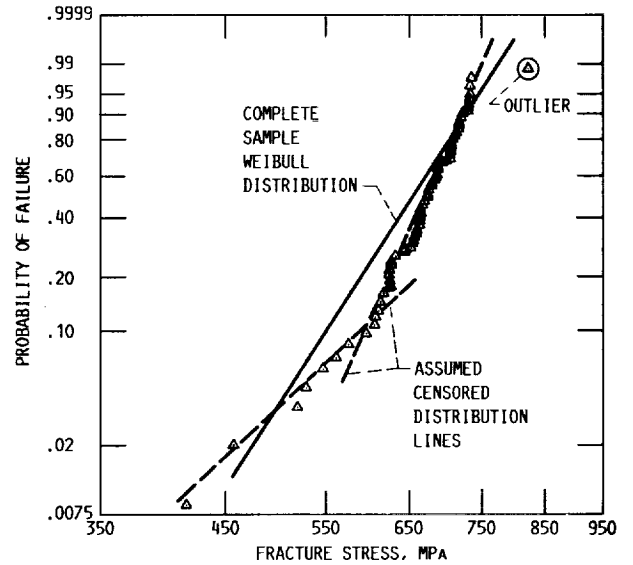


FIGURE 3. - COMPLETE SAMPLE AND ASSUMED CENSORED SAMPLE WEIBULL DISTRIBUTIONS, AND OUTLIER IN ASEA CERAMA HIPPED SILICON NITRIDE ( $Si_3N_4$ ). (FRACTURE STRESS DATA GENERATED AT NASA-LEWIS; NOT ALL DATA POINTS SHOWN.)

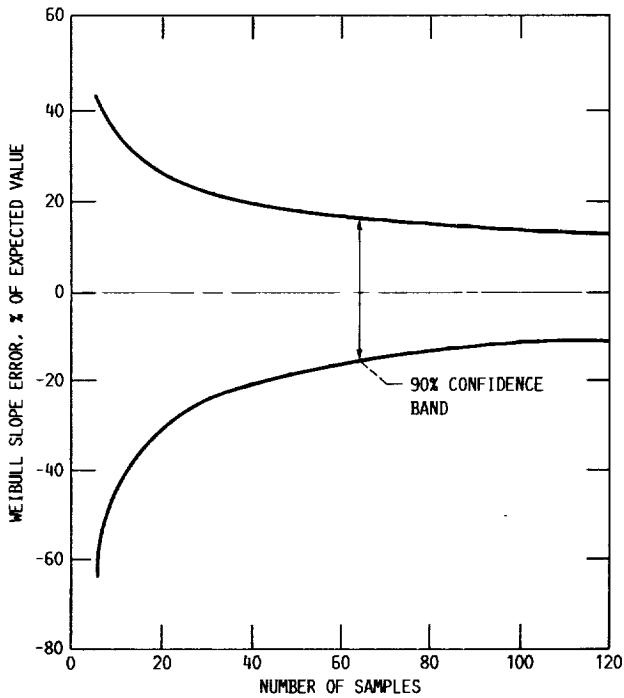


FIGURE 4. - WEIBULL SLOPE ERROR VERSUS SAMPLE SIZE.

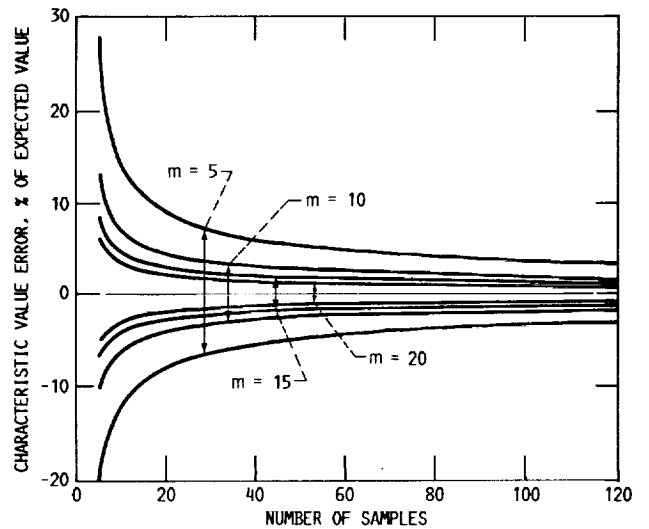


FIGURE 5. - CHARACTERISTIC VALUE ERROR VERSUS SAMPLE SIZE - 90% CONFIDENCE BANDS.

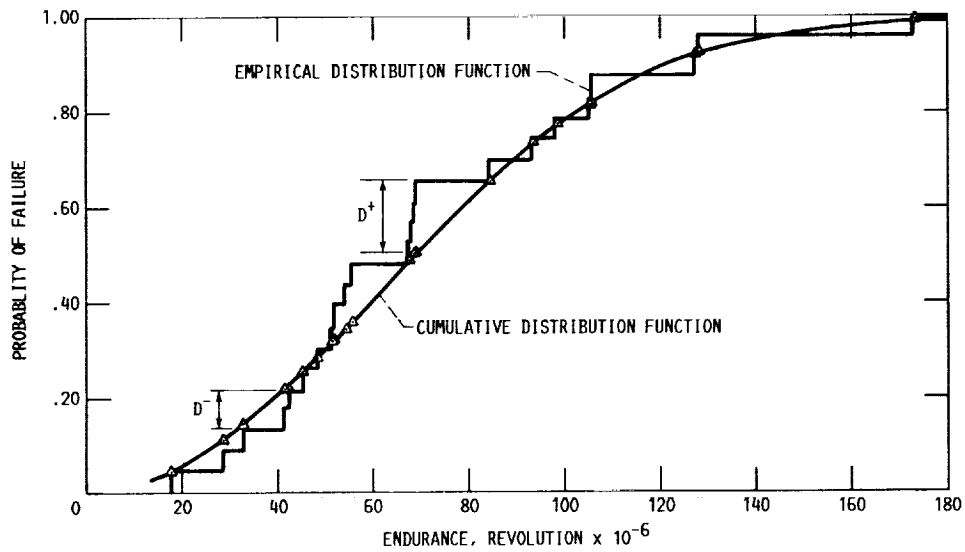


FIGURE 6. - EMPIRICAL DISTRIBUTION FUNCTION (EDF) OF DEEP-GROOVE BALL-BEARING ENDURANCE TESTS. (K-S STATISTIC  $D = D^+ = 0.1512$ .)

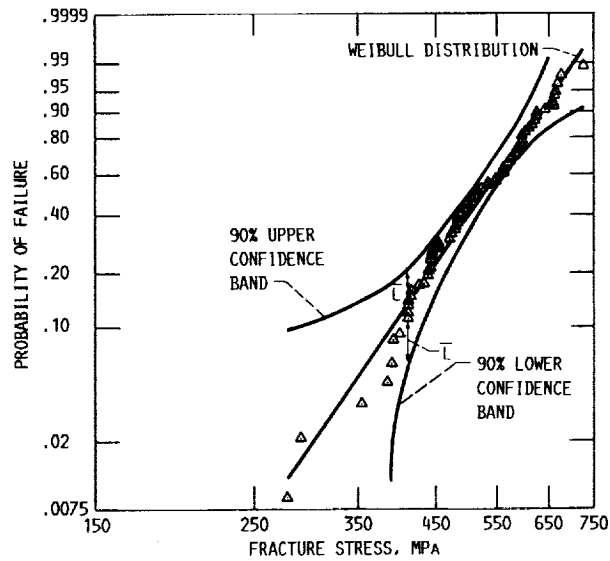


FIGURE 7. - 90-PERCENT CONFIDENCE BANDS ABOUT THE WEIBULL LINE FOR ESK HIPped SILICON CARBIDE (SiC). (FRACTURE STRESS DATA GENERATED AT NASA-LEWIS; NOT ALL DATA POINTS SHOWN;  $\bar{L} = 0.0829$ .)



1. Report No. NASA TM-100890		2. Government Accession No.		3. Recipient's Catalog No.	
4. Title and Subtitle Calculation of Weibull Strength Parameters and Batdorf Flow-Density Constants for Volume- and Surface-Flaw-Induced Fracture in Ceramics				5. Report Date October 1988	
				6. Performing Organization Code	
7. Author(s) Shantaram S. Pai and John P. Gyekenyesi				8. Performing Organization Report No. E-4128	
				10. Work Unit No. 505-63-1B	
9. Performing Organization Name and Address National Aeronautics and Space Administration Lewis Research Center Cleveland, Ohio 44135-3191				11. Contract or Grant No.	
				13. Type of Report and Period Covered Technical Memorandum	
12. Sponsoring Agency Name and Address National Aeronautics and Space Administration Washington, D.C. 20546-0001				14. Sponsoring Agency Code	
15. Supplementary Notes Portions of this material were presented at the Third International Symposium on Ceramic Materials and Components for Engines sponsored by the American Ceramic Society, Las Vegas, Nevada, November 27-30, 1988. Shantaram S. Pai, W. L. Tanksley and Associates, Inc., Lewis Research Center, Cleveland, Ohio 44135; John P. Gyekenyesi, NASA Lewis Research Center					
16. Abstract This paper describes the calculation of shape and scale parameters of the two-parameter Weibull distribution using the least-squares analysis and maximum likelihood methods for volume- and surface-flaw-induced fracture in ceramics with complete and censored samples. Detailed procedures are given for evaluating 90-percent confidence intervals for maximum likelihood estimates of shape and scale parameters, the unbiased estimates of the shape parameters, and the Weibull mean values and corresponding standard deviations. Furthermore, this paper describes the necessary steps for detecting outliers and for calculating the Kolmogorov-Smirnov and the Anderson-Darling goodness-of-fit statistics and 90-percent confidence bands about the Weibull distribution. It also shows how to calculate the Batdorf flaw-density constants by using the Weibull distribution statistical parameters. The techniques described have been verified with several example problems from the open literature, and have been coded in the Structural Ceramics Analysis and Reliability Evaluation (SCARE) design program.					
17. Key Words (Suggested by Author(s)) Ceramic strength; MOR bars; Weibull parameters; Least squares; Maximum likelihood; Outliers; Confidence bands; Complete and censored data; Goodness-of-fit; Batdorf; Flaw density constants, SCARE				18. Distribution Statement Unclassified - Unlimited Subject Category 39	
19. Security Classif. (of this report) Unclassified		20. Security Classif. (of this page) Unclassified		21. No of pages 32	22. Price* A03

